Quantification of the tidal exchange of radium as an indicator of submarine groundwater inputs to Great South Bay.

A Thesis Presented

by

Suhui Yang

to

The Graduate School

in Partial fulfillment of the

Requirements

for the Degree of

Master of Science

in

Marine and Atmospheric Science

Stony Brook University

May 2008

Stony Brook University

The Graduate School

Suhui Yang

We, the thesis committee for the above candidate for the
Master of Science degree,
Hereby recommend acceptance of this thesis.

Henry J. Bokuniewicz, Professor
School of Marine and Atmospheric Science
Stony Brook University

J. Kirk Cochran, Professor
School of Marine and Atmospheric Science
Stony Brook University

Robert E. Wilson, Associate Professor
School of Marine and Atmospheric Science
Stony Brook University

This thesis is accepted by the Graduate School

Lawrence Martin

Dean of the Graduate School

Abstract of the Thesis

Quantification of the tidal exchange of radium as an indicator of submarine groundwater inputs to Great South Bay

by

Suhui Yang

Master of Science

in

Marine and Atmospheric Science

Stony Brook University

2008

Concentrations of short-lived radium isotopes were measured in Fire Island Inlet, Great South Bay, NY over a spring tidal cycle. When combined with available water fluxes from a numerical hydrodynamic model, these provide an independent assessment of the exchange of radium through the inlet, the predominant term in a radium budget for Great South Bay used, in turn, to calculate submarine groundwater discharge (SGD). The flux of ^{223}Ra could balance with the other known inputs and outputs, without the need of a radium input via SGD. Using ^{224}Ra an additional input of radium from SGD is required to balance the radium budget in the bay but the value is less than a previous estimate. The differences show the need to better resolve the terms in a radium budget used to calculate SGD and highlight inherent uncertainties in the method.

Table of Contents

List of Figures

List of Tables

Acknowledgments

This work was supported by the Korea Research Foundation Grant funded by the Korea government (MOEHRD) (KRF-2005-215-C00136).

1. Introduction

Natural geochemical tracers, like radium, have been used to estimate groundwater discharge rates in many settings (Moore, 1996; Rama and Moore, 1996; Moore, 2000; Kelly and Moran, 2002). The use of groundwater tracers has an advantage that they present an integrated signal as they enter the water column via various pathways in an aquifer (Burnett et al., 2006). On the other hand, it is sometimes difficult to know the sources and sinks of the tracers that are necessary for a mass balance.

Radium, a naturally-occurring radioelement, is enriched in groundwater compared to seawater (Rama and Moore, 1996; Moore, 1997). Four radium isotopes, ^{223}Ra, ^{224}Ra, ^{226}Ra, and ^{228}Ra, belong to the uranium-thorium decay series. They are continuously produced by the decay of insoluble, thorium parents in sediments. While thorium is usually tightly bound to sediment particles, radium behaves differently. Radium is bound to sediment grains in freshwater, but becomes readily desorbable from sediments by ion exchange with other dissolved cations as sediments are flushed with saline water (Webster et al., 1994; Hancock and Murray, 1996; Moore, 1997; Hancock et al., 2000). Excess radium in coastal waters may come from radium desorbed from suspended riverine sediments, radium regenerated or released from bottom sediments, and radium carried in by groundwater (Burnett and Tai, 1992; Moore, 1997; Hancock et al, 2000; Kelly and Moran, 2002).

With half-lives of ^{223}Ra, ^{224}Ra, ^{226}Ra, and ^{228}Ra: 11.4 days, 3.6 days, 5.7 years, and 1600 years, respectively, the short-lived Ra isotopes (^{223}Ra and ^{224}Ra) are more useful in evaluating coastal mixing rates (Moore, 2000; Burnett and Dulaiova, 2003; Purkl and

Eisenhauer, 2004; Moore, 2006) and average residence times in estuaries (Moore, 1996; Kelly and Moran, 2002). The long-lived Ra isotopes (^{226}Ra and ^{228}Ra) are applied to quantify groundwater fluxes in that these give an index of the SGD fluxes as they regenerate slowly and are conservative tracers (Rama and Moore, 1996; Moore, 1998; Hwang et al., 2005; Moore, 2006).

In this study, I measured the tidal flux of radium into and out of a large lagoon, Great South Bay, on the south shore of Long Island, NY, through its principal inlet (Fire Island Inlet). As I will discuss, an earlier study of a radium budget in Great South Bay (Beck et al., 2007b) found that tidal exchange through Fire Island Inlet was the dominant term in the radium budget. The objective of my research was therefore to better quantify this important component of the radium budget and its implications for the amount of submarine groundwater discharge (SGD) into Great South Bay.

1.1. Site description

Great South Bay is an approximately 45 km long and 11 km wide estuary, which is located along the south shore of Long Island, New York, USA (Bokuniewicz, 1991). The surface area is approximately 2.1×10^8 m^2, and the average mean low water depth is 1.3 m (Bokuniewicz, 1991; Wilson et al., 1991; Kenneth, 2005). The two largest streams that drain into the bay are the Carmens and Connetquot rivers. Their combined discharge is 1.5×10^8 L d^{-1}. Tidal range in the bay is generally less than about 0.25 m, and the semidiurnal tidal prism is 5.2×10^{10} L (Beck et al., 2007b). Water flow in and out of the bay is restricted by Fire Island as a barrier, and the entire system is vertically well mixed. In the bay, fresh waters from Long Island and minor amounts from Fire Island dilute the salinity of the bay measurably. The most direct pathway for water exchange between the bay and Atlantic Ocean is Fire Island Inlet. The inlet varies in width from 0.8 to 1.2 km, with depth ranging from 2.0 to 7.6 m. The tidal current up to 70 cm s^{-1} exists in the inlet while the central and eastern Great South Bay has very weak tidal current (5 cm s^{-1}; Wong, 1993).

Great South Bay is one of the most productive estuaries in the world (Lively et al., 1983) and brown tide blooms have been experienced periodically, every year since the late spring or summer of 1985 (Cosper et al., 1987; Bricelj and Lonsdale, 1997; LaRoche et al., 1997; Nuzzi and Waters, 2004). Nuzzi and Waters (2004) suggested that groundwater inputs to the bay may be a factor in controlling dissolved inorganic nitrogen (DIN), an excess of which can lead to algal blooms.

1.2. Previous work

The past measurement of submarine groundwater discharge (SGD) into Great South Bay (Bokuniewicz and Zeitlin, 1980) was done using vented, benthic chambers (Lee, 1977) at six locations along the shore. By extrapolation of direct measurements near the shoreline, a total input of SGD was estimated to be $3.6 – 4.7 \times 10^9$ L d^{-1}.

I have recently participated in the construction of a radium budget for Great South Bay based on measurements of the four radium isotopes (Beck et al., 2007b). Thirty-six open water samples were collected over the whole Great South Bay as well as two major rivers into the bay, the Carmens and the Connetquot rivers. At the mouth of the Connetquot River, another seven samples were measured to estimate Ra input by water percolation through marshes. During six hours from high to low tide, the Ra activities tended to be linear with salinity, resulting in the conclusion that there was no or little marsh contribution (Beck et al., 2007b). Similar to the marsh input, there was evidence of a little Ra contribution from desorption from river-borne and resuspended sediments, as also indicated in Jamaica Bay, another lagoon on Long Island. Indeed, desorption accounted for less than 2 % of the total Ra input (Beck et al., 2007a). In addition, the contribution of Ra by diffusion from fine-grained sediments was investigated using sediment cores (Beck et al., 2007a). In each core, the overlying water was replaced with Ra free bay water for various time intervals, ranged 0 and 400 hours. The incubated water was drained and analyzed for dissolved Ra. After that, new Ra free water was filled with the core again. Three time measurements were done for a single core, and 6 – 8 % of total Ra input resulted from this diffusion term.

These measurements were then combined in a mass balance:

$$J_{out} + J_{decay} = J_{in} + J_{Car} + J_{Conn} + J_{marsh} + J_{desorp} + J_{diff} + J_{SGD},$$

where Ra loss from the bay occurred through water exchange at the inlet (J_{out}) and radioactive decay (J_{decay}). The Ra input into the bay was controlled by several terms: water exchange at the inlet (J_{in}), river run-off from Carmans and Connetquot River (J_{Car} and J_{Conn}), water percolation through fringing marshes (J_{marsh}), desorption from river-borne and resuspended sediments (J_{desorp}), diffusion from fine-grained sediments (J_{diff}), and submarine groundwater discharge (J_{SGD}). All estimated fluxes were shown in the Table 1. As explained, fluxes from marshes and desorption have little contribution, so that the terms, J_{marsh} and J_{desorp}, were ignored in the mass balance. The flux imbalance was 0.97×10^9 dpm d^{-1} for ^{223}Ra and 24.5×10^9 dpm d^{-1} for ^{224}Ra, meaning that these must be the magnitude of J_{SGD}, the only unknown term.

Beck et al. (2007b) reached two important conclusions. First, the radium budget revealed a major imbalance, with an unaccounted-for source representing 32 – 57 % of the total Ra input. This unknown input was attributed to discharge of brackish groundwater with high Ra activities. Applying the Ra activities measured in shallow groundwater in Great South Bay, the SGD flux was estimated to be between 3.5 and 4.5 $\times 10^9$ L d^{-1} (Table 1). The second important conclusion was that the largest terms in the radium mass balance were those from radium exchange through Fire Island Inlet, representing 35 – 67 % of the total Ra input, and 67 – 100% of the export (Beck et al., 2007b). In order to estimate Ra influx through the inlet (J_{in}), Beck et al. (2007b) used the radium concentration in three ocean-end member samples (0.61 dpm 100 L^{-1} for ^{223}Ra and 14.4 dpm 100 L^{-1} for ^{224}Ra) and a tidal prism of 1.05×10^{11} L d^{-1}. Ra flux out of the bay (J_{out}) was estimated as the product of the tidal prism and the average radium concentration in the bay (1.40 dpm 100 L^{-1} for ^{223}Ra and 27.4 dpm 100 L^{-1} for ^{224}Ra; Beck et al., 2007b). In my study, I endeavored to measure these important Ra fluxes (J_{in} and J_{out}) directly at a station in Fire Island Inlet, in order to investigate the resolution of these terms and consequent uncertainties in the radium budget.

2. Methods

Over a tidal cycle, 60 L water samples from 1 m below the surface and 1 m above the bottom were pumped every hour. Twenty-four samples were taken in all. All samples were passed through MnO_2-impregnated acrylic fiber columns (4.5 cm diameter, 25 cm length) at a flow rate less than 1 L min^{-1} (Yamada and Nozaki, 1986; Yang et al., 1992). Upon collecting samples, salinity was recorded promptly by YSI probe which simultaneously measures pH, temperature, and salinity (Webster et al., 1995). Also, triplicate measurements of current were recorded every 30 minutes by "Ott" current meter at 2.5 m below surface. This position in the water column was approximately 0.7 of the water depth which, empirically, should represent the depth-averaged velocity (Rahn, 1996).

To quantify the short-lived radium isotopes (^{223}Ra and ^{224}Ra), each Mn-fiber sample was partially dried (Sun and Torgersen, 1998) and placed in an air circulation system, described by Moore and Arnold (1996). Helium gas is circulated over the Mn-fiber to sweep radon daughters of ^{223}Ra and ^{224}Ra into a scintillation detector where alpha decay of Rn and Po occurs. The signals from the detector are routed to a delayed coincidence counter (DCC). DCC uses the difference in decay constants of polonium daughters to identify alpha particles from ^{219}Rn and ^{220}Rn, and therefore to determine activities of ^{223}Ra and ^{224}Ra.

In order to calculate Ra flux in and out at the inlet, we used volume flux of water from a tidal model, called FVCOM. FVCOM is a prognostic, unstructured-grid, finite-volume, free-surface, 3–D primitive equation coastal ocean circulation model developed jointly by researchers at the University of Massachusetts and at Woods Hole Oceanographic Institute (Chen et al., 2003). FVCOM was originally developed for the estuarine flooding/drying process in estuaries and the tidal-, buoyancy-, and wind-driven circulation in the coastal region featured with complex irregular geometry and steep bottom topography. In particular, FVCOM provides prediction of the depth-averaged current velocity at my station as well as the total flux of water through a cross-section of Fire Island Inlet where my station was located. These are given as a curve of current velocity and discharge of water volume throughout the inlet versus time. By comparison of the predicted current speeds from the model with the currents measured in the station, the modeled tidal volume fluxes are adjusted to the proper tidal phase during sampling, getting the best estimate of water volume flux during sampling period.

3. Results

3.1. Salinity and currents at Fire Island Inlet

Sample collection was conducted near the Robert Moses Causeway at Fire Island Inlet (40°37.8’ N, 73°14.8’ W) during 28 June 2007 at time of spring tide (Fig. 1). The approximate width of the inlet here was 0.93 km. During the sampling period, the depth measured was about 5.6 m, on average. The water column was well-mixed throughout the period. Salinity data is shown in Table 2. While the average salinity in Great South Bay is

27 (Beck et al., 2007b), the average surface salinity measured at the inlet over the period was 33.6 which was the same of average bottom salinity. The pattern of changing salinity will be used later to determine the times of the flood-to-ebb and ebb-to-flood transitions. However, although the instrument had been calibrated, these salinities seem high. Offshore salinities of 31 are more typical. As I will discuss later, because the radium activities at the end of the flood tide were the same as the ocean end-member determined by Beck et al. (2007b), my measured salinities will later be adjusted to a maximum value of 31.

The measured current velocity ranged up to nearly 0.8 m s^{-1} which agreed well with tidal-model calculations. Sampling began on a flooding tide, continued through the full ebb and ended in the subsequent flood tide. Slack tide appears to have occurred around occurred at 8:30 AM (8.52 hour: flood to ebb) and again at 2:55 PM (14.92 hour: ebb to flood), although there was uncertainty in the exact time because currents were low for a considerable period. The measured time series of the current velocity were superimposed on the predicted, average velocity calculated by the model in order to choose the best tidal phase to represent the sampling period (Fig. 2). In the model calculation, this would be the period between the 62.10 and 74.52 hours; model times were later adjusted to match the actual sample time series. The calculated volume flux for this period ranged from – 2380.83 m^3 s^{-1} (out of the inlet) to 2804.21 m^3 s^{-1} (into the inlet) as shown in Fig. 3. The net volume flux over the 12.42 hour period was calculated to be 4.9×10^5 m^3 per tidal cycle out of the inlet, corresponding to a value of 9.5×10^8 L d^{-1}.

In this study, the sampling period was on June 28, 2007, and Beck et al. (2007b) collected samples during August 14 – 16, 2006; both periods were at time of spring tide. Nevertheless, the tidal prism calculated by the model from the ebb tide through Fire Island Inlet was slightly lower than the tidal prism previously used (Beck et al., 2007b). The estimated water volume over the ebb-period was calculated with the model to be 4.2×10^{10} L while a tidal prism of 5.2×10^{10} L was estimated in the prior investigation.

3.2. Dissolved Ra in water column at Fire Island Inlet

All samples represented saline end-members. At Fire Island Inlet, both short-lived Ra concentrations and salinities at surface water were similar at the bottom although surface ^{224}Ra activities tended to be slightly higher than at the bottom (Table 2). For example, average ^{224}Ra was 1.3 dpm 100 L^{-1} higher at the surface, but the trend was not consistent throughout the sampling period. The averages of ^{223}Ra and ^{224}Ra activities were 1.09 dpm 100 L^{-1} and 24.4 dpm 100 L^{-1}, respectively. As expected, these were higher than values typically found offshore; for example, values of < 0.3 dpm 100 L^{-1} for ^{223}Ra and < 0.5 dpm 100 L^{-1} for ^{224}Ra have been found at offshore of South Atlantic Bight (Moore, 2000).

The lowest radium activities which might be taken to represent an ocean end-member near slack tide between flood and ebb were about 0.50 dpm 100 L^{-1} for ^{223}Ra and 18.0 dpm 100 L^{-1} for ^{224}Ra (Fig. 4). Both of these values agree well with the ocean end-members found in the earlier study (Beck et al. 2007b). Highest radium activities were seen near the time of low tide (12:40 PM). The highest activities, which might represent the bay activities, were about 1.46 dpm 100 L^{-1} for ^{223}Ra and 30.2 dpm 100 L^{-1} for ^{224}Ra (Fig. 4).

Assuming the salinity near slack time (flood to ebb) showed the same salinity value which was used as an ocean end-member (Beck et al., 2007b), the measured highest salinity of 34.9 at the inlet was adjusted to 31. With this corrected salinity, Ra activities showed a linear relationship, resulting from physical mixing of radium-enriched bay water with the ocean (Fig. 5). Based on the linear relationship, at a typical bay salinity of 27, the Ra activities would be 1.84 dpm 100 L^{-1} for ^{223}Ra and 38.7 dpm 100 L^{-1} for ^{224}Ra. These estimates are higher compared to 1.40 dpm 100 L^{-1} and 27.4 dpm 100 L^{-1}, ^{223}Ra and ^{224}Ra, respectively, from the earlier study (Beck et al., 2007b).

4. Discussion

There are several ways to interpret these data to obtain values for the next radium flux through Fire Island Inlet. Previously, Beck et al. (2007b) had calculated fluxes into the bay to be 0.64×10^9 dpm d^{-1} and 15.1×10^9 dpm d^{-1} for ^{223}Ra and ^{224}Ra, respectively, while fluxes out of the bay were estimated to be 1.46×10^9 dpm d^{-1} for ^{223}Ra and 28.6×10^9 dpm d^{-1} for ^{224}Ra. The net imbalance at the inlet ($J_{out} - J_{in}$) was 0.82×10^9 dpm d^{-1} for ^{223}Ra and 13.5×10^9 dpm d^{-1} for ^{224}Ra, indicating these amounts are out of the bay through the inlet. This net imbalance combined in the mass balance, and then total Ra flux imbalance into the bay of 0.97×10^9 dpm d^{-1} for ^{223}Ra and 24.5×10^9 dpm d^{-1} for ^{224}Ra was given simply using this equation; $J_{SGD} = J_{decay} + (J_{out} - J_{in}) - (J_{Car} + J_{Conn} + J_{diff})$. These values can be compared to estimates calculated from the data presented below.

4.1. A direct Ra flux calculation

Water volume flux was calculated at time of spring tide by the model, and result for the appropriate tidal cycle between 62.10 and 74.52 hours of the simulation was shown (Fig. 3). I interpolated the calculated model fluxes at a time interval of 0.01 hours over a 12.42 hour tidal cycle, and multiplied those values by the average radium concentration. The difference of Ra activities between the surface and bottom values at any particular sampling time gave uncertainties about the average values ranging from 0 % to 9.7 % for ^{223}Ra and 0.3 % to 6 % for ^{224}Ra. The average radium concentration (one-half the sum of the surface concentration and the bottom concentration) was assumed constant from the midpoint in time between the two successive samples (Fig. 6 and 7).

The fluxes into Great South Bay were calculated as 0.97×10^9 dpm d^{-1} for ^{223}Ra and 21.3×10^9 dpm d^{-1} for ^{224}Ra (Table 3). The fluxes out of the bay were estimated as 0.80×10^9 dpm d^{-1} for ^{223}Ra and 18.1×10^9 dpm d^{-1} for ^{224}Ra. These were both comparable to those calculated by Beck et al. (2007b) but the influxes were larger than the previous estimates and the outfluxes were smaller. Both produced a radium imbalance at the inlet of 0.17×10^9 dpm d^{-1} for ^{223}Ra and 3.26×10^9 dpm d^{-1} for ^{224}Ra, indicating these amounts come into the bay. Hereafter, all other terms for Ra source and sink are assumed to be same as Beck et el. (2007b) measured. With the given numbers, the total Ra imbalance into the bay was given as $– 0.06 \times 10^9$ dpm d^{-1} for ^{223}Ra and 7.7×10^9 dpm d^{-1} for ^{224}Ra.

4.2. Estimate based on the flood-ebb activity differences

Another way to interpret these data is to recognize the difference between the low Ra activity from the ocean and the elevated Ra activity in the bay as documented in the radium measurements at the inlet that I discussed in the results. The difference between the ocean activity (low values on the radium cycle; Fig. 4) and the bay activity (high values on the radium cycle; Fig. 4) might be taken to represent the enrichment of radium in the bay. This would be 0.96 dpm 100 L^{-1} for ^{223}Ra and 12.2 dpm 100 L^{-1} for ^{224}Ra. If this excess is carried out by the net outflow of water (9.5×10^8 L d^{-1}), the result would be a loss of radium from the bay to the ocean of 0.009×10^9 dpm d^{-1} for ^{223}Ra and 0.12×10^9 dpm d^{-1} for ^{224}Ra. Both values are substantially smaller than those estimated earlier but these fluxes are out of the bay (from the bay to the ocean) as expected. These numbers were put in the mass balance and it resulted in the total Ra imbalance into the bay of 0.12×10^9 dpm d^{-1} for ^{223}Ra and 11.1×10^9 dpm d^{-1} for ^{224}Ra.

4.3. Bay end-member estimate

A third estimate might be made by extrapolating the linear relation between the corrected salinity and radium activities (Fig. 5) to the average bay salinity of 27. These might be taken as the average Ra activity of bay water, and flux out at the inlet was calculated as a product of the average bay Ra activity and the net water flux through the inlet. Performing this extrapolation, the activity of ^{223}Ra at a salinity of 27 would be 1.84 dpm 100 L^{-1}, compared to a value of 1.40 dpm 100 L^{-1} from Beck et al. (2007b). For ^{224}Ra the value was 38.7 dpm 100 L^{-1} compared to a value of 27.4 dpm 100 L^{-1} from Beck et al. (2007b). Multiplying these values by the net water outflow gives ^{223}Ra value of 0.017×10^9 dpm d^{-1} and ^{224}Ra value of 0.37×10^9 dpm d^{-1} out of the bay through the inlet. These are comparable to, but smaller than the original estimates of Beck et al. (2007b). Also, the total Ra imbalance was given as 0.13×10^9 dpm d^{-1} for ^{223}Ra and 11.3×10^9 dpm d^{-1} for ^{224}Ra into the bay.

4.4. Adjustment to the calculation of the direct Ra fluxes

Since the radium activities in the bay are elevated over the ocean, and the net water flow is out of the bay, the direct calculation of a net influx of radium from the ocean was not to be expected. The net flux calculated in this way is a small difference between two large numbers, and it may be that measurements made at one point in the inlet do not adequately represent the actual flux through the entire cross-section; small, perhaps random, fluctuations in any of the parameters may unduly affect the results. Lateral mixing especially near slack tide may be affecting the results. In addition, some fraction of the water that flows out of the inlet in the ebb tide returns to the bay on the subsequent flood. This is confirmed by the lag between the variations in radium concentrations and the flood-ebb cycle (Fig. 4). It is parameterized as a tidal exchange ratio, R, which is the ratio of new ocean water and the total amount of water that enters the bay on a flood tide. In principle, R can be estimated using the salinity measurements (Fischer et al. 1979, p.265). The highest salinity was expected to appear at the slack (flood to ebb) and the lowest at slack time from ebb to flood (Fig. 8).

In the face of all the difficulties previously mentioned, the following, four-step procedure was used to recalculate the direct radium flux.

1. A curve comprised of the dominant semidiurnal tidal period (M_2) and one, shallow-water harmonic (M_4) was fit to the measured salinities (Fig. 9; R. Wilson, 2007, Marine Sciences Research Center, personal communication). I then adjusted the ebb-flood transition times of the modeled volume fluxes to match the times indicated by the salinity measurements by linear interpolation.

2. Next, a tidal curve consisting of three components (M_2, M_4, and M_6) was fitted to model results (R. Wilson, 2007, Marine Sciences Research Center, personal communication). Then with a percentage correction factor, I adjusted the magnitude of the newly timed, flood and ebb volume fluxes to reproduce a net volume of 4.9×10^5 m^3 and a total ebb volume of 4.2×10^7 m^3 as calculated initially with the model.

3. The salinity was adjusted to a maximum value of 31 as discussed above, and the flux of salinity was calculated every 0.01 hour over a tidal cycle as the product of the adjusted salinity from the fitted curve (step 3) and the (time and magnitude) adjusted water-volume fluxes (steps 2 and 3). The average salinity of the water leaving on the ebb tide was found to be 29.7755. This quantity referred to as "S_e" by Fischer et al. (1979), and yielded an R value of 0.287.

4. Radium activity was calculated from the salinity using the linear regressions shown in Fig. 5, and the net radium fluxes were calculated as the product of this activity and the (time and magnitude) adjusted water-volume fluxes (steps 2 and 3). This calculation yielded a net flux of ^{223}Ra out of the inlet, as expect, at a magnitude of 0.01 × 10^9 dpm d^{-1}. The net flux of ^{224}Ra was still into the inlet but at a lower rate of 0.46 × 10^9 dpm d^{-1}. These net fluxes then resulted in the total Ra imbalance of 0.12 × 10^9 dpm d^{-1} for ^{223}Ra and 10.5 × 10^9 dpm d^{-1} for ^{224}Ra into the bay.

4.5. Implications for SGD

One goal of constructing a radium budget in Great South Bay is the calculation of submarine groundwater discharge (SGD). SGD was previously calculated to be 4.5 × 10^9 L d^{-1} using ^{223}Ra, and 3.5 × 10^9 L d^{-1} using ^{224}Ra (Beck et al. 2007b). These are expected to be maximum values because the smallest Ra activity was used as ocean end-member for estimating the influx (J_{in}). In order to put my new measurements of radium at Fire

Island Inlet in the context of SGD, I would assume that the other sources and sinks remain the same as determined by Beck et al. (2007b). Both studies were done in the summer season at time of spring tide, although in different years. Combining the results in this way is not intended to provide a better estimate of SGD, but merely to show the sensitivity of the calculation to the inlet flux. All the values in the discussion to follow are summarized in Table 4.

My direct Ra flux calculation through the inlet had a net flux of ^{223}Ra into the bay at a rate of 0.17×10^9 dpm d^{-1} (or – 0.17×10^9 dpm d^{-1} out of the bay). This value can be combined with the previously determined sources and sinks to give a total, small flux imbalance for the entire bay of – 0.06×10^9 dpm d^{-1} (Table 4). In this case since, according to my direct calculation, more ^{223}Ra enters the bay through all mechanisms than leaves. Theoretically, this would require a negative SGD but the values are so low near zero, assuming that the ^{223}Ra budget can be balanced without the necessity of ^{223}Ra input from SGD. So, a minimum value for SGD would be zero. I do not interpret this to mean that SGD was actually zero, but that the uncertainties in the flux estimate through the inlet were too great to resolve the SGD input. Adjusting the calculation of the direct ^{223}Ra flux, as described in Section 4.4, yielded a net Ra outflux, as we might have expected, but corresponding to an estimated SGD of only 0.57×10^9 L d^{-1}, a value one-eighth of that estimated by Beck et al. (2007b). To support it with the other estimates I have discussed, net ^{223}Ra fluxes of 0.009×10^9 dpm d^{-1} (section 4.2) and of 0.017×10^9 dpm d^{-1} (section 4.3) through the inlet yield the total flux imbalance of 0.12 and 0.13×10^9 dpm d^{-1}, respectively that correspond to the SGD estimate of 0.57×10^9 L d^{-1} and 0.62×10^9 L d^{-1}.

The direct measurement of the ^{224}Ra flux through the inlet yielded a value of 3.26×10^9 dpm d^{-1} for the net flux of radium; this was also into the bay. However, when combined with the previous estimates of the sources and sink, the result is an imbalance in the bay as a whole of 7.7×10^9 dpm d^{-1} which corresponds to a SGD of 1.1×10^9 L d^{-1} or about one-third of the previous estimate. Adjusting the calculation of the direct ^{224}Ra flux as described in Section 4.4, still yielded a net Ra influx, but a small one, corresponding to an estimated SGD of 1.5×10^9 L d^{-1}, a value about 40% of that estimated by Beck et al. (2007b). The other estimates result in the net fluxes of ^{224}Ra of 0.12×10^9 dpm d^{-1} (section 4.2) and of 0.37×10^9 dpm d^{-1} (section 4.3) through the inlet results in the total flux imbalance of 11.1 and 11.4×10^9 dpm d^{-1}, respectively. Both correspond to the highest estimate of SGD of 1.6×10^9 L d^{-1}, about one-half the original estimate (table 4).

5. Conclusion

The largest term in the radium budget for Great South Bay is the tidal exchange through Fire Island Inlet. In an effort to assess the sensitivity of results to estimates of these Ra fluxes, the radium budget in Great South Bay has been recalculated using direct measurements of concentration of ^{223}Ra and ^{224}Ra over a tidal cycle. The results are comparable to earlier measurements but, when carried through to the calculation of SGD have shown a maximum estimate of SGD that is only a half of the earlier value for ^{224}Ra

and within the natural variability and uncertainty of the measurements, could be consistent with no SGD at all for ^{223}Ra. This exercise demonstrates the need to better resolve the major fluxes of radium if the technique is to be used, with accuracy, for quantitative estimates of SGD.

6. References

Beck, A. J., John, P. R., Cochran, J. K., and Bokuniewicz, H. J., 2007a, Radium mass-balance in Jamaica Bay, NY: Evidence for a substantial flux of submarine groundwater, Marine Chemistry, 106, p. 419-441.

Beck, A. J., John, P. R., Cochran, J. K., Bokuniewicz, H. J., and Yang, S., 2007b, Submarine groundwater discharge to Great South Bay, NY, estimated using Ra isotopes, Marine Chemistry, submitted.

Bokuniewicz, H. J. and Zeitlin, M. J., 1980, Characteristics of groundwater seepage into Great South Bay. Marine Science Research Center, Special Report 35, SUNY, Stony Brook, NY, 30 p.

Bokuniewicz, H. J., 1991, The origin and development of the Great South Bay: a geological perspective, In: Schubel, J. R., Bell, T. M., Carter, H. H. (Eds.), The Great South Bay. State University of New York Press, Albany, New York, p. 5-8.

Bricelj, V. M. and Lonsdale, D. J., 1997, Aureococcus anophagefferens: Causes and ecological consequences of brown tides in U.S. mid-Atlantic coastal waters, Limnology and Oceanography, 42, p. 1023-1038.

Burnett, W. C., Aggarwal, P. K., Bokuniewicz, H., Cable, J. E., Charette, M. A., Kontar, E., Krupa, S., Kulkarni, K. M., Loveless, A., Moore, W. S., Oberdorfer, J. A., Oliveira, J., Ozyurt, N., Povinec, P., Privitera, A. M. G., Rajar, R., Ramessur, R. T., Scholten, J., Stieglitz, T., Taniguchi, M., and Turner, J. V., 2006, Quantifying Submarine Groundwater Discharge in the Coastal Zone via Multiple Methods, Science of the Total Environment, 367, p. 498-543.

Burnett, W. C. and Dulaiova, H., 2003, Estimating the dynamics of groundwater input into the coastal zone via continuous radon-222 measurements, Journal of Environmental Radioactivity, 69, p. 21-35.

Burnett, W. C. and Tai, W. C., 1992, Determination of radium in natural-waters by alpha liquid scintillation, Analytical Chemistry, 64, p. 1691-1697.

Chen, C., Liu, H. and Beardsley, R. C., 2003, An unstructured grid, finite-volume, three-dimensional, primitive equations ocean model: Application to coastal ocean and estuaries, Journal of Atmospheric and Oceanic Technology, 20, p. 159-186.

Cosper, E. M., Dennison, W. C., Carpenter, E. J., Bricelj, V. M., Mitchell, J. G., Kuenstner, S. H., Colflesh, D., and Dewey, M., 1987, Recurrent and persistent brown tide blooms perturb coastal marine ecosystem, Estuaries, 10, p. 284-290.

Fischer, H. B., List, J. E., Koh, C. R., Imberger, J., and Brooks, N. H., 1979, Mixing in Inland and Coastal Waters, Academic Press, NY: 483 pp.

Hancock, G. J. and Murray, A. S., 1996, Source and distribution of dissolved radium in the Bega River estuary, Southeastern Australia, Earth and Planetary Science Letters, 138, p. 145-155.

Hancock, G. J., Webster, I. T., Ford, P. W., and Moore, W. S., 2000, Using Ra isotopes to examine transport processes controlling benthic fluxes into a shallow estuarine lagoon, Geochimica et Cosmochimica Acta, 64, p. 3685-3699.

Hwang, D. W., Kim, G., Lee, Y. W., and Yang, H. S., 2005, Estimating submarine inputs of groundwater and nutrients to a coastal bay using radium isotopes, Marine Chemistry, 2005, 96, p. 61-71.

Kelly, R. P. and Moran, S. B., 2002, Seasonal changes in groundwater input to a well-mixed estuary estimated using radium isotopes and implications for coastal nutrient budgets, Limnology and Oceanography, 47, p. 1796-1807.

Kenneth, R. H., 2005, Water quality and ecology of Great South Bay, Fire Island National Seashore Science Synthesis Paper, Technical Report NPS/NER/NRTR—2005/019: 54 pp.

LaRoche, J., Nuzzi, R., Waters, R., Wyman, K., Falkowski, P., and Wallace, D., 1997, Brown tide blooms in Long Island's coastal waters linked to interannual variability in groundwater flow, Global Change Biology, 3, p. 397-410.

Lee, D. R., 1977, A device for measuring seepage flux in lakes and estuaries, Limnology and Oceanography, 25, p. 183-186.

Lively, J. S., Kaufman, Z., and Carpenter, E. J., 1983, Phytoplankton ecology of a barrier island estuary: Great South Bay, New York, Estuarine, Coastal, and Shelf Sciences, 16, p. 51-68.

Moore, W. S., 1996, Large groundwater inputs to coastal waters revealed by 226Ra enrichments, Nature, 380, p. 612-614.

Moore, W. S., 1997, High fluxes of radium and barium from the mouth of the Ganges-Brahmaputra River during low river discharge suggest a large groundwater source, Earth and Planetary Science Letters, 150, p. 141-150.

Moore, W. S., 1998, Application of Ra-226, Ra-228, Ra-223, and Ra-224 in coastal waters to assessing coastal mixing rates and groundwater discharge to oceans, Proceeding of The Indian Academy of Sciences-Earth and Planetary Sciences, 107, p. 343-349.

Moore, W. S., 2000, Determining coastal mixing rates using radium isotopes, Continental Shelf Research, 20, p. 1993-2007.

Moore, W. S., 2006, The role of submarine groundwater discharge in coastal biogeochemistry, Journal of Geochemical Exploration, 88, p. 389-393.

Moore, W. S. and Arnold, R., 1996, Measurement of 223Ra and 224Ra in coastal waters using a delayed coincidence counter, Journal of Geophysical Research, 101, p. 1321-1329

Nuzzi, R. and Waters, R. A., 2004, Long-term perspective on the dynamics of brown tide blooms in Long Island coastal bays, Harmful Algae, 3, p. 279-293.

Purkl, S. and Eisenhauer, A., 2004, Determination of radium isotopes and Rn-222 in a groundwater affected coastal area of the Baltic Sea and the underlying sub-sea floor aquifer, Marine Chemistry, 87, p. 137-149.

Rama and Moore, W. S., 1996, Using the radium quartet for evaluating groundwater input and water exchange in salt marshes, Geochimica et Cosmochimica Acta, 60, no. 23, p. 4645-4652.

Rahn, P. H., 1996, Engineering Geology: an environmental approach, Prentice Hall, Saddle River NJ: 657 pp.

Sun, Y. and Torgersen, T., 1998, The effects of water content and Mn-fiber surface conditions on 224Ra measurement by 220Rn emanation, Marine Chemistry, 62, p. 299-306.

Webster, I. T., Hancock, G. J., and Murray, A. S., 1994, On the use of radium isotopes to estimate sediment flushing rates in an estuary, Limnology and Oceanography, 38, p.1917-1927.
Webster, I. T., Hancock, G. J., and Murray, A. S., 1995, Modeling the effect of salinity on radium desorption from sediments, Geochimica et Cosmochimica Acta, 59, p. 2469-2476.

Wilson, R. E., Wong, K. C., and Carter, H. H., 1991, Aspects of circulation and exchange in Great South Bay, In: Schubel, J. R., Bell, T. M., Carter, H. H. (Eds.), The Great South Bay. State University of New York Press, Stony Brook, New York, p. 9-22.

Wong, K. C., 1993, Numerical simulation of the exchange process within a shallow bar-built estuary, Estuaries, 16, p. 335-345.

Yamada, M. and Nozaki, Y., 1986, Radium isotopes in coastal and open ocean surface waters of the western North Pacific, Marine Chemistry, 19, p. 379-389.

Yang, H. S., Kwon, Y. A., Kim, G. B., and Kim, S. S., 1992, Distributions of 226Ra and 228Ra in the surface waters of East Sea of Korea, Bulletin of the Korean Fisheries Society, 25, p. 399-405.

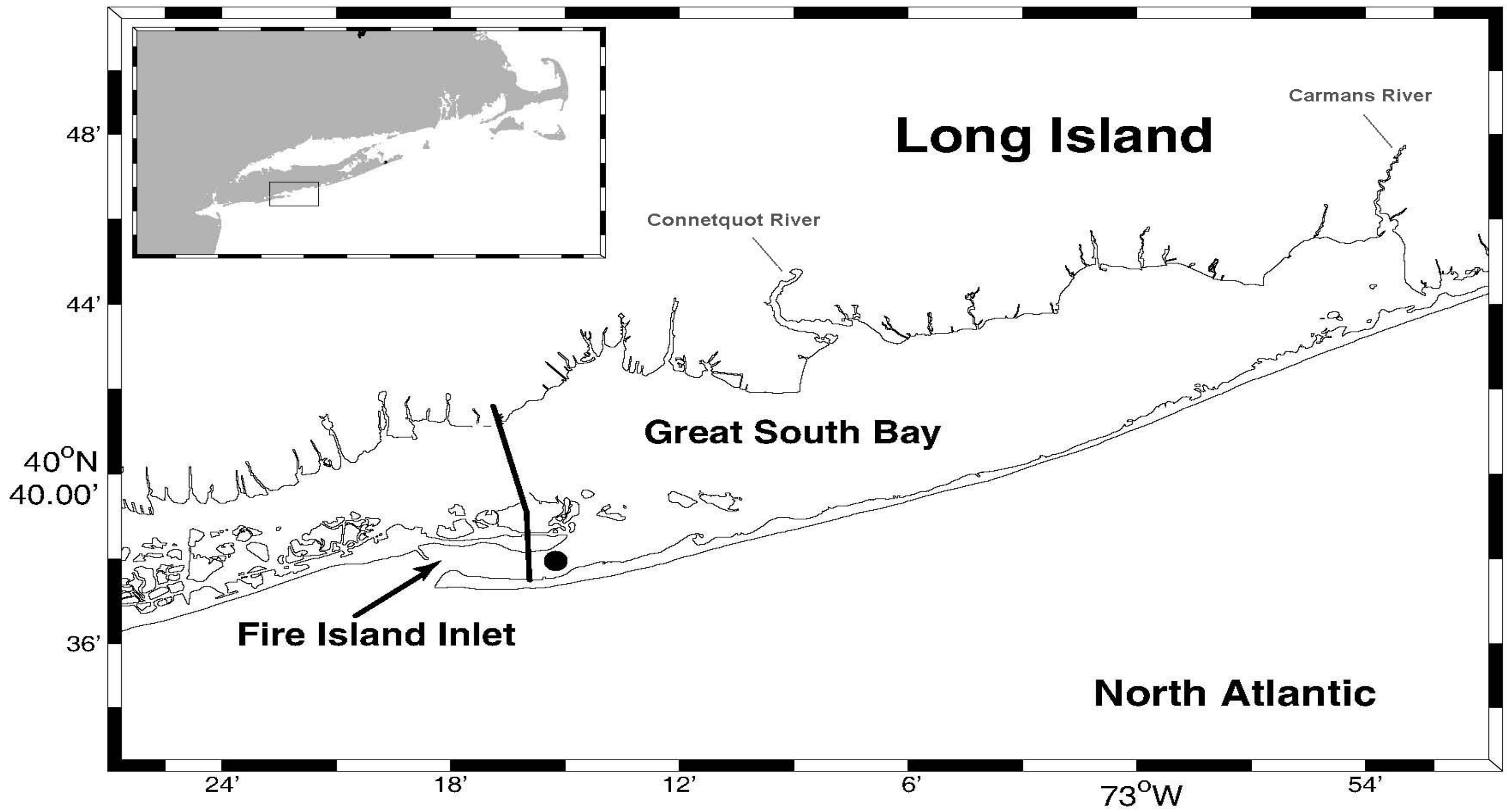

Figure 1. Great South Bay, NY. Sampling station at Fire Island Inlet is marked with solid circle (40°37.8' N, 73°14.8' W). The solid line across Great South Bay indicates Robert Moses Causeway.

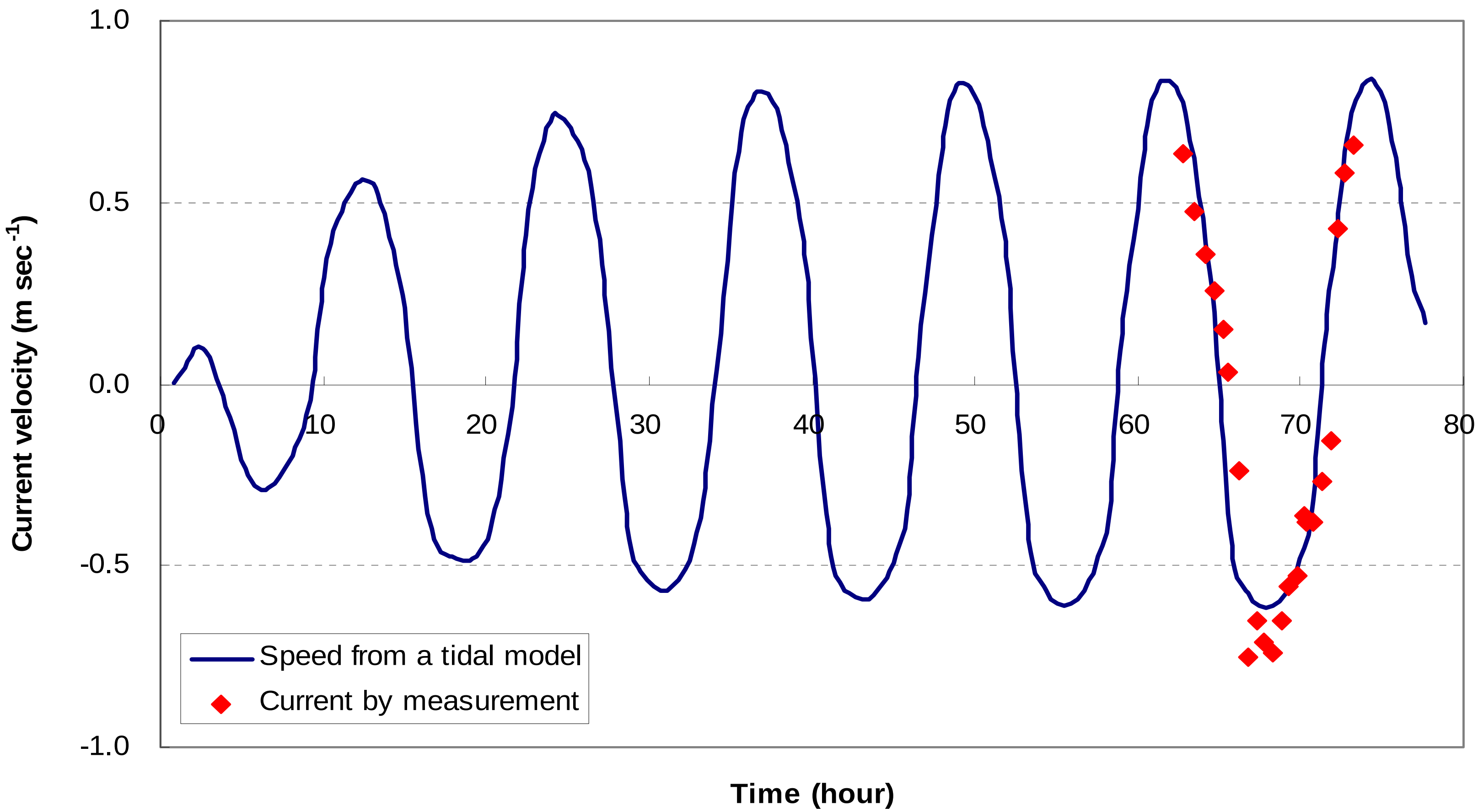

Figure 2. Match of speed by a tidal model with current by measurement. Solid line represents speed from the model, and dots show current from measurement.

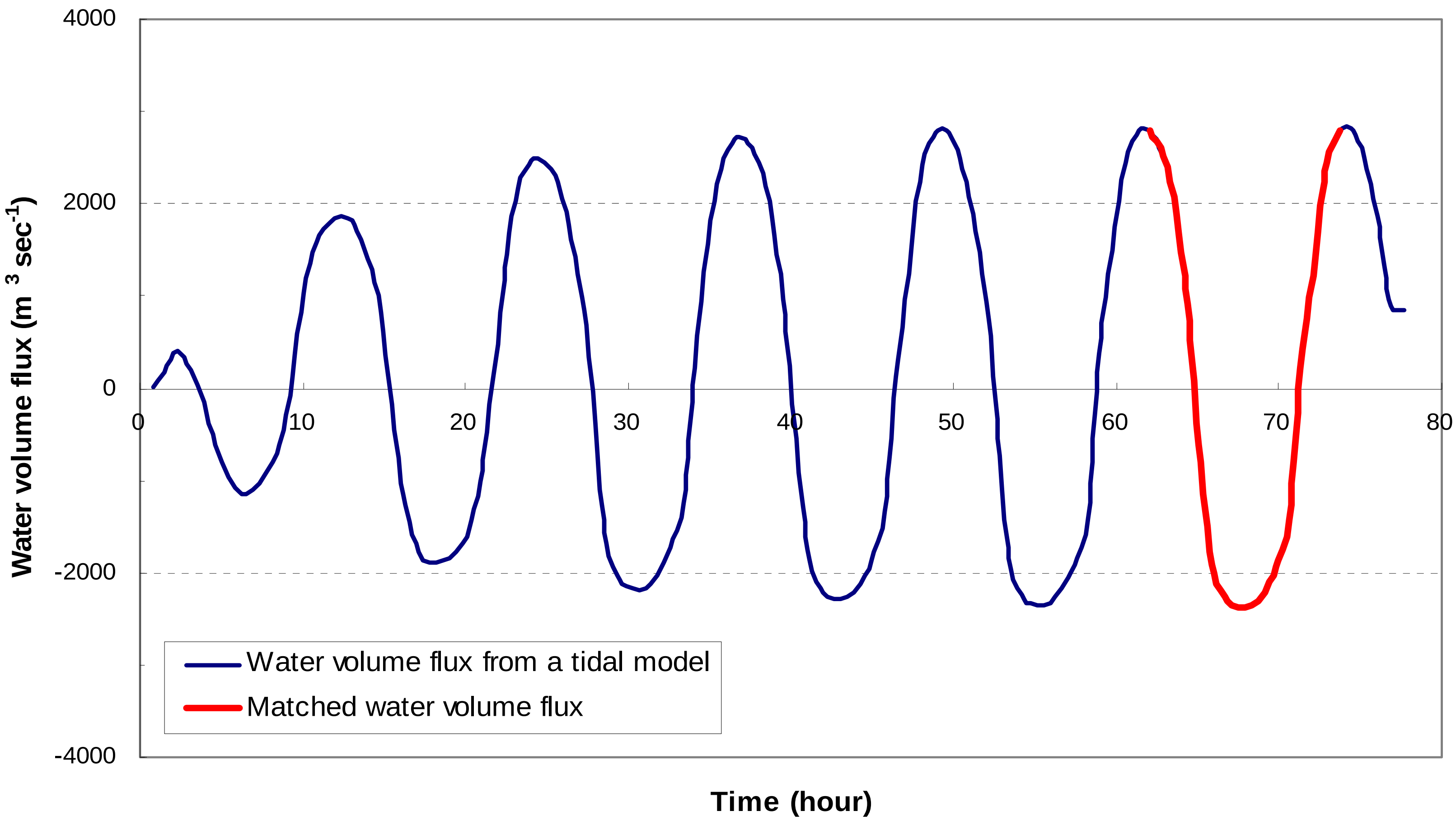

Figure 3. Matched water volume flux estimated by a tidal model at time of right tidal cycle (62.10 – 74.52 of model time).

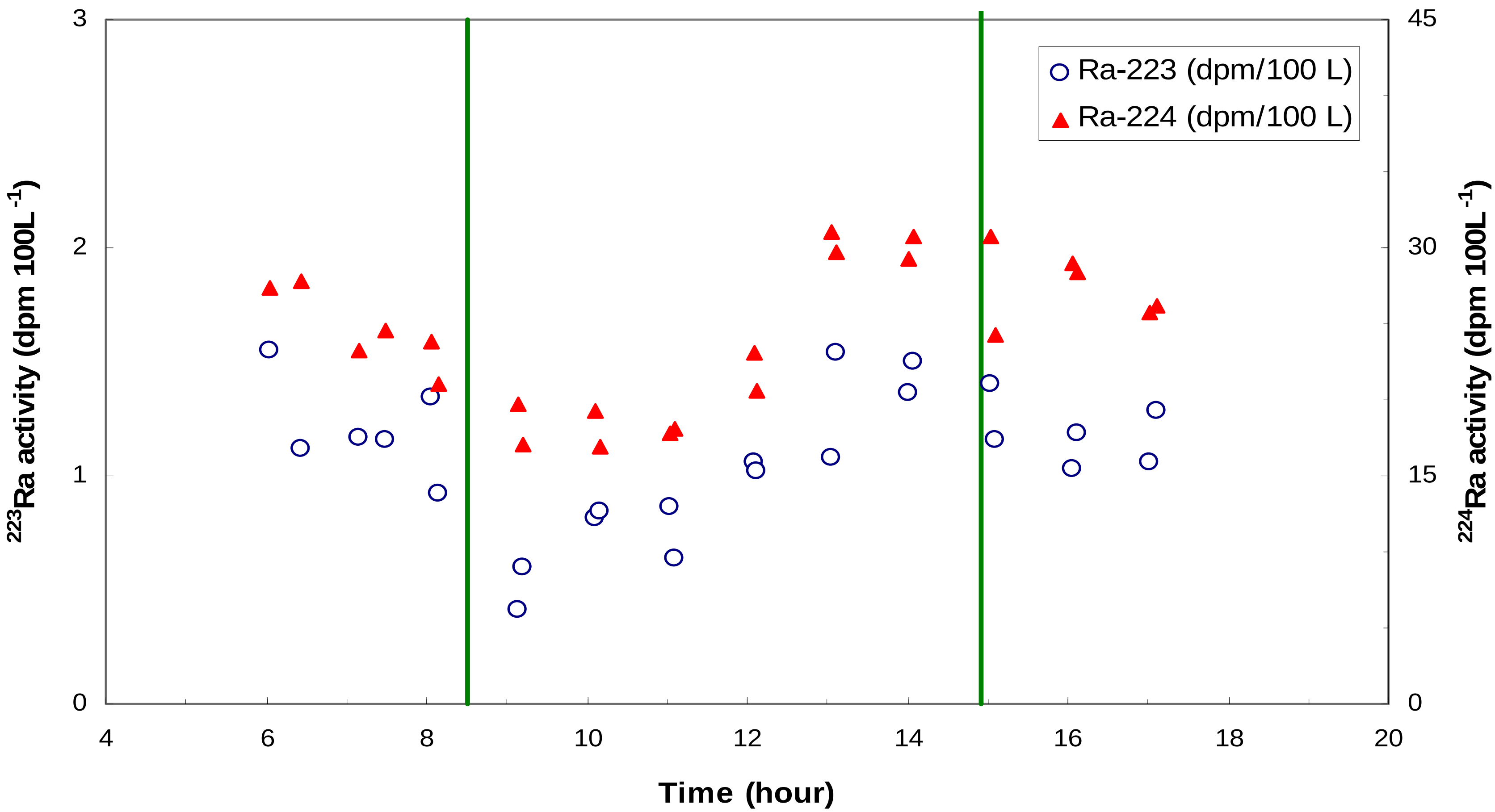

Figure 4. ^{223}Ra and ^{224}Ra activities trends with sampling time. Hollow and filled ones represent ^{223}Ra and ^{224}Ra, respectively. The two solid lines classify flood, ebb, and flood time in order.

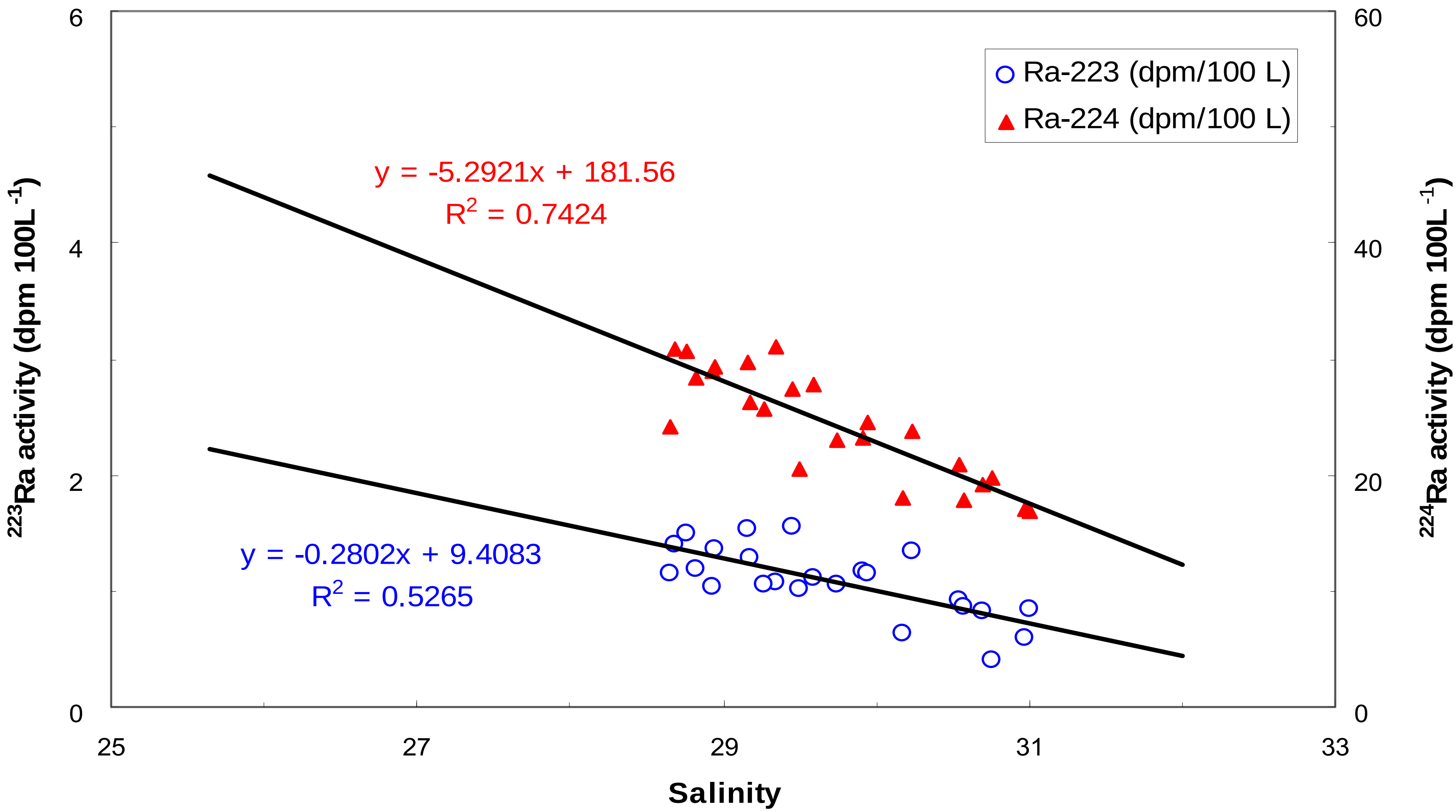

Figure 5. Relationship between ^{223}Ra and ^{224}Ra activities and the corrected salinity. Solid lines show a linear regression of the data for each isotope; best fit equations and correlation coefficients are also shown.

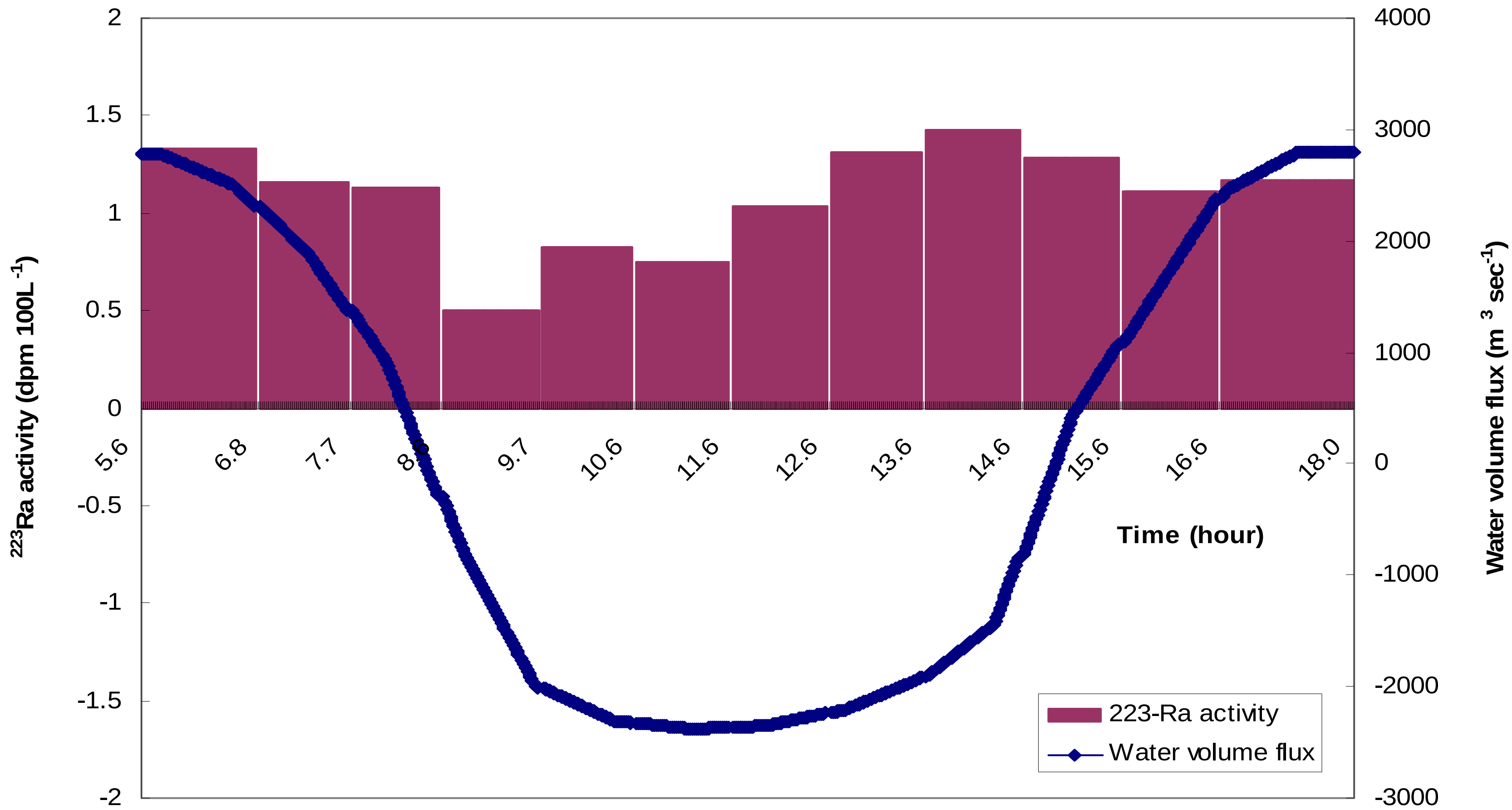

Figure 6. ^{223}Ra flux trend with time. Bar indicates the average ^{223}Ra activity of surface and bottom at time. Solid line shows the water volume flux during the sampling period. Time series is indicated over 0.01 hour.

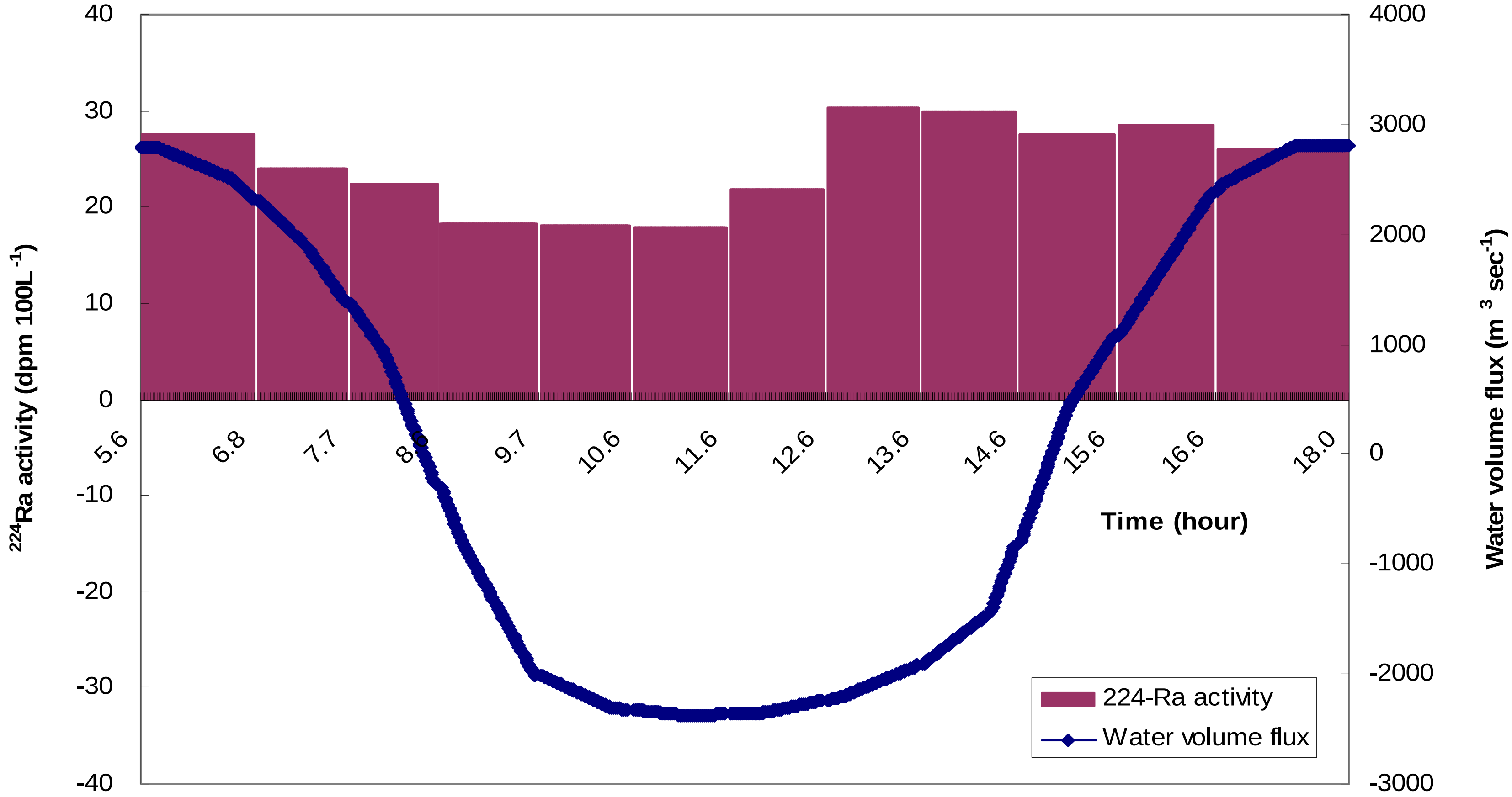

Figure 7. ^{224}Ra flux trend with time. Bar indicates the average ^{224}Ra activity of surface and bottom at time. Solid line shows the water volume flux during the sampling period. Time series is indicated over 0.01 hour.

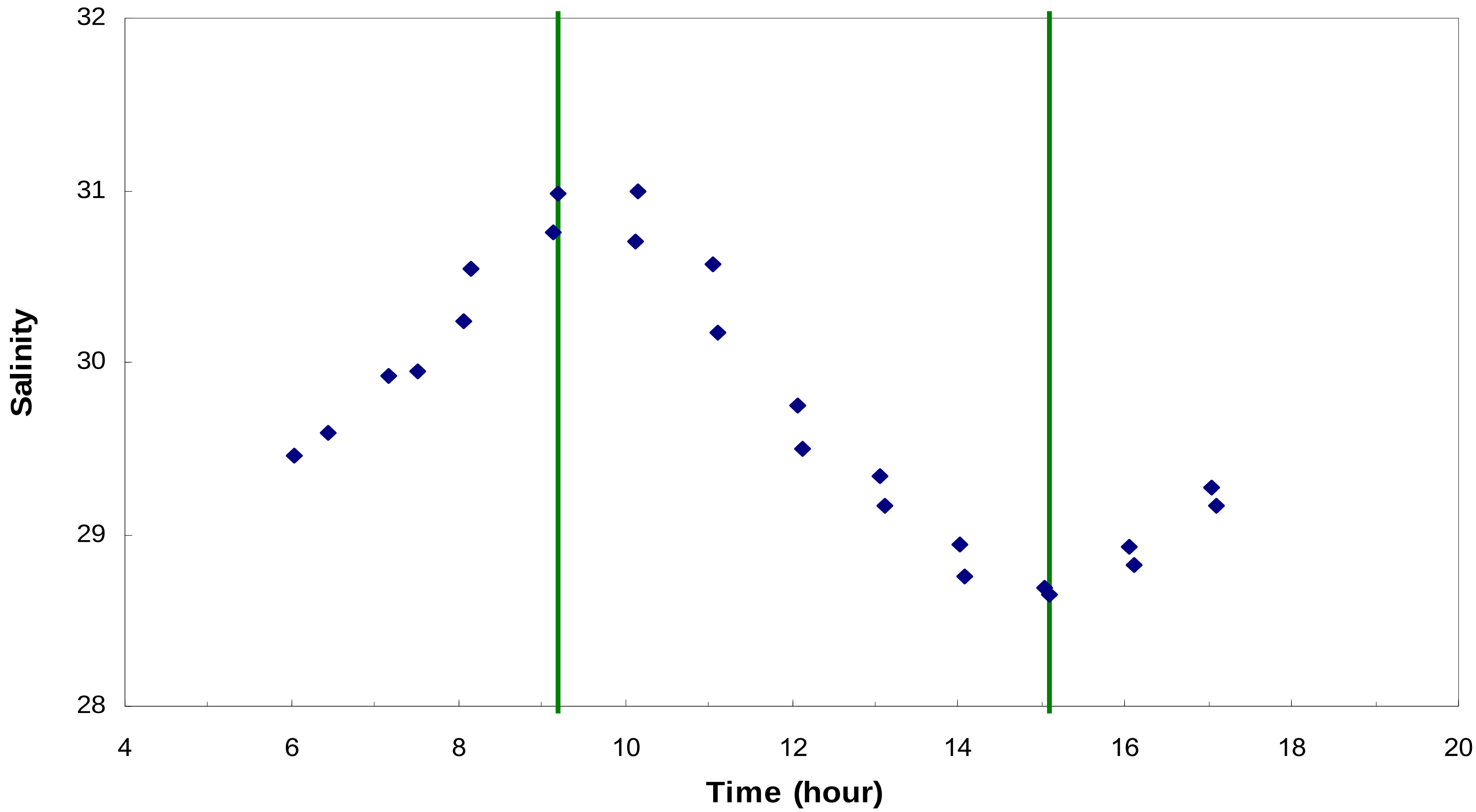

Figure 8. Corrected salinity of all water samples changes with time. The left solid line delineate flood from ebb, and the right line ebb from flood.

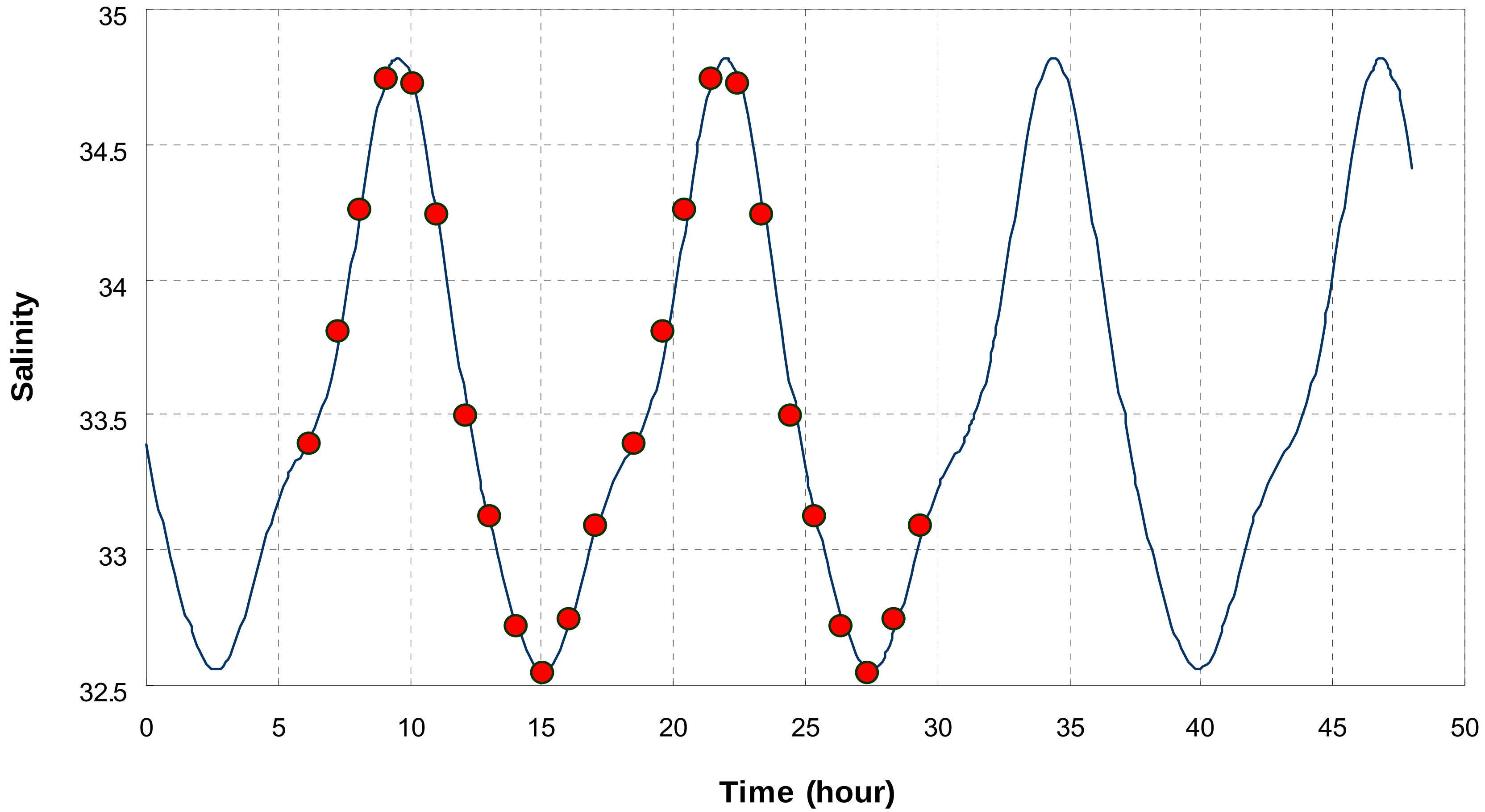

Figure 9. Tidal curve (M_2 and M_4) fit to the salinity data (R. Wilson, 2007, Marine Sciences Research Center, personal communication). Salinity values would later be adjusted to a maximum value of 31 (see text).

	Fluxes into Great South Bay (10^9 dpm d^{-1})					Fluxes out of the bay (10^9 dpm d^{-1})				
	Carmans River	Connetquot River	Diffusion	Ocean exchange	Sum input	Ocean exchange	Decay	Sum removal	Flux imbalance (10^9 dpm d^{-1})	SGD (10^9 L d^{-1})
^{223}Ra	0.002	0.004	0.11	0.64	0.72	1.46	0.23	1.69	0.97	4.5
^{224}Ra	0.021	0.053	3.3	15.1	18.4	28.6	14.33	43.0	24.5	3.5

Table 1. Estimated Ra fluxes in Great South Bay for August 2006 (Beck et al., 2007b).

Sample ID	Salinity	^{223}Ra dpm100L^{-1}	^{224}Ra dpm100L^{-1}
FII-1S	33.5	1.1 ± 0.08	27.7 ± 0.04
FII-1D	33.3	1.5 ± 0.07	27.4 ± 0.03
FII-2S	33.8	1.2 ± 0.12	23.3 ± 0.05
FII-2D	33.8	1.2 ± 0.10	24.5 ± 0.05
FII-3S	34.1	1.3 ± 0.09	23.9 ± 0.04
FII-3D	34.4	0.9 ± 0.09	21.0 ± 0.04
FII-4S	34.6	0.4 ± 0.14	19.7 ± 0.07
FII-4D	34.9	0.6 ± 0.14	17.1 ± 0.07
FII-5S	34.6	0.8 ± 0.13	19.2 ± 0.06
FII-5D	34.9	0.8 ± 0.12	16.8 ± 0.06
FII-6S	34.4	0.9 ± 0.08	17.8 ± 0.04
FII-6D	34.0	0.6 ± 0.07	18.1 ± 0.03
FII-7S	33.6	1.1 ± 0.05	23.0 ± 0.02
FII-7D	33.4	1.0 ± 0.04	20.6 ± 0.02
FII-8S	33.2	1.1 ± 0.08	31.0 ± 0.04
FII-8D	33.0	1.5 ± 0.07	29.6 ± 0.04
FII-9S	32.8	1.4 ± 0.09	29.3 ± 0.04
FII-9D	32.6	1.5 ± 0.07	30.7 ± 0.04
FII-10S	32.6	1.4 ± 0.12	30.8 ± 0.06
FII-10D	32.5	1.2 ± 0.12	24.2 ± 0.06
FII-11S	32.8	1.0 ± 0.10	28.9 ± 0.05
FII-11D	32.7	1.2 ± 0.09	28.4 ± 0.05
FII-12S	33.1	1.1 ± 0.18	25.7 ± 0.09
FII-12D	33.0	1.3 ± 0.16	26.2 ± 0.08

Table 2. Ra activities and salinities of surface (S) and deep (D) water samples at Fire Island Inlet. Salinity values would later be adjusted to a maximum value of 31 (see text).

	Fluxes into the bay (10^9 dpm d^{-1})					Fluxes out of the bay (10^9 dpm d^{-1})				
	Carmans River	Connetquot River	Diffusion	Ocean exchange	Sum input	Ocean exchange	Decay	Sum removal	Flux imbalance (10^9 dpm d^{-1})	SGD (10^9 L d^{-1})
^{223}Ra	0.002	0.004	0.11	0.97	1.09	0.80	0.23	1.03	– 0.06	– 0.28
^{224}Ra	0.021	0.053	3.3	21.33	24.7	18.07	14.33	32.4	7.7	1.1

Table 3. New radium fluxes into Great South Bay with new ocean exchange values that measured directly at Fire Island Inlet for June 28, 2007.

Ra isotope	Basis of estimate (section)	Net outflux at the inlet (10^9 dpm d^{-1}) $J_{out} - J_{in}$	Flux imbalance (10^9 dpm d^{-1}) $J_{SGD} = J_{decay} + (J_{out} - J_{in}) - (J_{car} + J_{conn} + J_{diff})$	Est. SGD (10^9 L d^{-1})
^{223}Ra	Beck et al. (2007b)	0.82	0.97	4.5
	Direct measurement (4.1)	– 0.17	– 0.06	< 0
	Adjusted direct flux (4.4)	0.01	0.12	0.57
	Flood-ebb activity (4.2)	0.009	0.12	0.57
	Bay endmember (4.3)	0.017	0.13	0.62
^{224}Ra	Beck et al. (2007b)	13.5	24.5	3.5
	Direct measurement (4.1)	– 3.26	7.7	1.1
	Adjusted direct flux (4.4)	– 0.46	10.5	1.5
	Flood-ebb activity (4.2)	0.12	11.1	1.6
	Bay endmember (4.3)	0.37	11.3	1.6

Table 4. Comparison of all Ra flux estimates and implications for the estimate of SGD.